Cell Metabolism
Article

# The Ubiquitin Ligase Mul1 Induces Mitophagy in Skeletal Muscle in Response to Muscle-Wasting Stimuli

Sudarsanareddy Lokireddy,[1] Isuru W. Wijesoma,[1] Serena Teng,[1] Sabeera Bonala,[1] Peter D. Gluckm[illegible]
Craig McFarlane,[2] Mridula Sharma,[3,*] and Ravi Kambadur[1,2,*]
[1]School of Biological Sciences, Nanyang Technological University, Singapore 637551, Singapore
[2]Singapore Institute for Clinical Sciences (A*STAR), Brenner Centre for Molecular Medicine, 30 Medical Drive, Singapore 117609, Singapore
[3]Department of Biochemistry, YLL School of Medicine, National University of Singapore, Singapore 117[illegible], Singapore
*Correspondence: bchmridu@nus.edu.sg (M.S.), kravi@ntu.edu.sg (R.K.)
http://dx.doi.org/10.1016/j.cmet.2012.10.005



## SUMMARY

Recent research reveals that dysfunction and subsequent loss of mitochondria (mitophagy) is a potent inducer of skeletal muscle wasting. However, the molecular mechanisms that govern the deregulation of mitochondrial function during muscle wasting are unclear. In this report, we show that different muscle-wasting stimuli upregulated mitochondrial E3 ubiquitin protein ligase 1 (Mul1), through a mechanism involving FoxO1/3 transcription factors. Overexpression of Mul1 in skeletal muscles [illegible]yoblast cultures was sufficient for the induction of mitophagy. Consistently, Mul1 suppression not only protected against mitophagy but also partially rescued the muscle wasting observed in response to muscle-wasting stimuli. Importantly, upregulation of Mul1, while increasing mitochondrial fission, resulted in ubiquitination and degradation of the mitochondrial fusion protein Mfn2. Collectively, these data explain the molecular basis for the loss of mitochondrial number during muscle wasting.

## INTRODUCTION

Skeletal muscle wasting arises either from primary myopathies, namely muscular dystrophy, or as a secondary symptom associated with cancer, AIDS, sepsis, obesity, aging, and diabetes (Dodson et al., 2011; Emery, 2002; Evans, 2010; Lecker, 2003). Earlier studies conducted on wasting skeletal muscles have identified that overstimulation of the ubiquitin-proteasome pathway promotes the loss of myofibrillar proteins (Bodine et al., 2001; Clarke et al., 2007; Cohen et al., 2009; Lokireddy et al., 2011a, 2011b). Unlike the ubiquitin-proteasome pathway, the role of the autophagy-lysosome pathway in skeletal muscle is less understood. However, reports have confirmed that the autophagy-lysosome pathway is critical for maintaining physiological skeletal muscle mass, as deletions in important autophagy-related proteins result in skeletal muscle dysfunction (Masiero et al., 2009). Importantly, inhibition of autophagy also promotes the accumulation of nuclear abnormalities, reduces cell viability, and disrupts [illegible]tion of mitochondria (O'Leary and Hood, 2009; Park et al., [illegible]). Furthermore, impaired lysosome-dependent degradation causes myopathies like Pompe and Danon diseases (Temiz et al., 2009). Conversely, elevated autophagy-lysosome pathway activity also results in myofibrillar and mitochondrial protein degradation (Bechet et al., 2005).

FoxO transcription factors, downstream targets of the IGF-1/Akt pathway, regulate the ubiquitin-proteasome system in response to skeletal muscle-wasting stimuli, including starvation, denervation, and exposure to glucocorticoids such as dexamethasone (Bodine et al., 2001; Sandri et al., 2004). Recent work has also demonstrated that Myostatin, a TGF-β superfamily member involved in the negative regulation of skeletal muscle growth and development, activated FoxO transcription factors in murine and human myotubes, which in turn enhanced ubiquitin-proteasome system activity and promoted muscle wasting (Kambadur et al., 1997; Lee and McPherron, 2001; Lokireddy et al., 2011a, 2011b; McFarlane et al., 2006; Zhou et al., 2010). FoxO3 has also been shown to induce the transcription of numerous genes involved with the autophagy-lysosome pathway, such as LC3, Atg7, Bnip3, Cathepsin L, and Gabarap1, in response to starvation and denervation, further implicating FoxO transcription factors as master regulators of the skeletal muscle-wasting program (Mammucari et al., 2007; Romanello et al., 2010; Zhao et al., 2007).

Enhanced activity of FoxO transcription factors has also been associated with disruption of mitochondrial function and organization (Romanello et al., 2010). Furthermore, mitochondrial dysfunction leads to impaired skeletal muscle function and development (Chen et al., 2010; Romanello et al., 2010). Perturbations in the structure, number, and function of mitochondria have also been linked to neuropathy and several metabolic diseases (Chen et al., 2007, 2010; Romanello et al., 2010; Youle and Narendra, 2011). For example, mitochondrial fusion proteins, namely mitofusin 2 (Mfn2), which is critical for maintenance and genomic stability of mitochondrial DNA (mtDNA) (Chen et al., 2010), were repressed in skeletal muscles isolated from both obese and nonobese diabetic patients (Bach et al., 2003; Lin et al., 2005; Soriano et al., 2006). Additionally, mutations in Parkin, an E3 ligase, and Pink1, a mitochondrial kinase that regulates Parkin function, are associated with impaired clearance of defective mitochondria, which in turn results in the onset of recessive Parkinson's disease (Gegg et al., 2010; Geisler et al., 2010).

Although significant efforts have unveiled numerous molecular candidates that regulate mitochondria function during metabolic and neuropathic disorders, the molecules that modulate mitochondrial number and activity during skeletal muscle wasting are not well known. In this report, we show that the mitochondrial ubiquitin ligase, Mul1 (mitochondrial E3 ubiquitin protein ligase 1), promotes the fragmentation, depolarization, and clearance of mitochondria through the autophagy-lysosome pathway during in vitro and in vivo skeletal muscle wasting. We further show that Mul1 overexpression during skeletal muscle wasting was mediated by FoxO3 and that the RING finger domain of Mul1 ubiquitinated and targeted Mfn2 for ubiquitin-proteasome-mediated degradation.

## RESULTS

### Dexamethasone, Myostatin, and Serum Starvation Perturbed Mitochondrial Architecture and Membrane Potential, and Promoted Mitochondrial DNA Depletion in C2C12 Cells

To assess mitochondrial organization during muscle wasting, we transfected C2C12 myoblasts with mtRed plasmid (Nakamura et al., 2006) and examined mitochondrial distribution upon exposure to Dex or hMstn or under serum starvation conditions. Control C2C12 myoblasts demonstrated elongated and [illegible] mitochondrial morphology, features characteristic of [illegible] mitochondria (Figure 1A). However, mitochondria appeared punctate and fragmented upon treatment with Dex or hMstn and during serum starvation (Figure 1A).

In addition to disrupting mitochondrial [illegible]ganization, Dex and hMstn also impaired mitochondrial activity as assessed through MitoTracker Red staining (see Figure S1A [illegible] Moreover, we noted decreased MitoTracker [illegible]d accumulation in C2C12 myoblasts and myotubes treated with Dex or hMstn (Figure S1B). Expectedly, C2C12 myoblasts and myotubes treated with Dex or hMstn or during serum [illegible]vation underwent marked depolarization after Oligomycin (5 μM) treatment as compared to control C2C12 myoblasts and myotubes (Figure 1B and Figure S1C). Carbonyl cyanide 3-chlorophenylhydrazone (CCCP) causes rapid mitochondrial membrane depolarization. Consistent with this, a similar decrease in mitochondrial potential was observed in all the samples immediately after the addition of CCCP (Figure 1B and Figure S1C). In addition, Dex, hMstn, and serum starvation resulted in reduced mtDNA copy number per nuclear genome (nuDNA) (mtDNA:nuDNA) ratio in C2C12 myotubes (Figure 1C).

### Dex, hMstn, and Serum Starvation Enhanced Mul1 Expression

We next examined the expression of known regulators of mitochondrial dynamics in C2C12 myotubes exposed to Dex or hMstn, and during serum starvation conditions. *Fis1* and *Drp1*, which promote the fragmentation of mitochondria (Romanello et al., 2010), were upregulated in serum-starved, Dex- and hMstn-treated C2C12 myotubes (Figure 1D). While we observed no change in the mRNA expression of *Mfn2* (Figure 1D), a GTPase that coordinates mitochondrial fusion, we found significantly reduced Mfn2 protein levels in human primary myotubes (hMb15) and in C2C12 myotubes subjected to serum starvation or treatment with Dex or hMstn when compared to control (Figure 1E and Figure S1D). A similar decrease in Mfn2 protein level was observed in C2C12 myotubes and H9c2 rat cardiomyocytes treated with Mstn expressing CHO cell-conditioned media (CHO Mstn) (Figure 1F). We noted that *Mfn1* gene expression, a homolog of *Mfn2* also involved in mitochondria fusion, was elevated in C2C12 myotubes in response to treatment with hMstn and during serum starvation (Figure 1E); however, Mfn1 protein levels were unchanged in serum-starved, Dex- and hMstn-treated human primary myotubes (hMb15) although a slight increase was observed in C2C12 myotubes (Figure 1E and Figure S1D). A slight increase in Mfn1 protein levels was also observed in CHO Mstn-treated C2C12 myotubes and H9c2 cells (Figure 1F). In addition, *Bnip3*, a well-characterized facilitator of mitochondrial integrity and autophagy in skeletal muscle, was upregulated by 8-, 6-, and 3-fold in serum-starved, hMstn-treated, and Dex-treated C2C12 myotubes, respectively, when compared to the control (Figure 1D).

Mul1 is a recently discovered mitochondrial E3 ligase implicated in the fragmentation of mitochondria (Braschi et al., 2009; Li et al., 2008; Zhang et al., 2008). We observed the upregulation of *Mul1* expression by 5-, 4-, and 2.5-fold in serum-starved, hMstn-treated, and Dex-treated C2C12 myotubes, respectively (Figure 1D). Additionally, a dose-dependent increase in *Mul1* expression was observed in C2C12 myotubes and H9c2 cells exposed to increasing concentrations of hMstn (Figure S1E and S1F). A similar increase in Mul1 protein level was observed in serum-starved, Dex-treated, and hMstn-treated human primary (hMb15) and C2C12 myotubes (Figure 1E and Figure S1D). Immunoblot analysis further confirmed increased Mul1 protein levels in C2C12 myotubes and H9c2 cells challenged with CHO Mstn (Figure 1F). Along with *Mul1*, we also noted increased expression of additional mitochondrial E3 ligases, namely *March5* and *Park2*, and the kinase *Park6*, upon exposure to hMstn and during serum starvation (Figure 1D).

### FoxO Transcription Factors Regulate Mul1 Expression

Analysis of the human and mouse *Mul1* gene promoters (2 kb), for putative skeletal muscle-wasting-associated transcription factor binding motifs (Table S1) (Sandri et al., 2004), revealed six putative FoxO transcription factor-binding sites in the human Mul1 promoter (Figure 2A). Importantly, FoxO transcription factors are involved in enhancing the ubiquitin-proteasome and autophagy-lysosomal pathways during skeletal muscle wasting (Mammucari et al., 2007; Romanello et al., 2010; Sandri et al., 2004; Zhao et al., 2007). To determine if FoxO transcription factors regulate *Mul1* gene expression, a 2 kb Mul1-Luc promoter-reporter construct and plasmids that express wild-type FoxO1 (WT-FoxO1), constitutively active FoxO1 (ca-FoxO1), wild-type FoxO3 (WT-FoxO3), or constitutively active FoxO3 (ca-FoxO3) were cotransfected into C2C12 myoblasts and then differentiated into myotubes. Increased Mul1 promoter activity was observed in the presence of ca-FoxO1 and ca-FoxO3 when compared to empty vector control (Figure 2A). WT-FoxO1- and WT-FoxO3-dependant Mul1 promoter-reporter activity was significantly elevated when compared to empty vector control, but lower when compared to the Mul1 promoter-reporter activity detected upon transfection with constitutively active FoxO1 or FoxO3, respectively (Figure 2A).

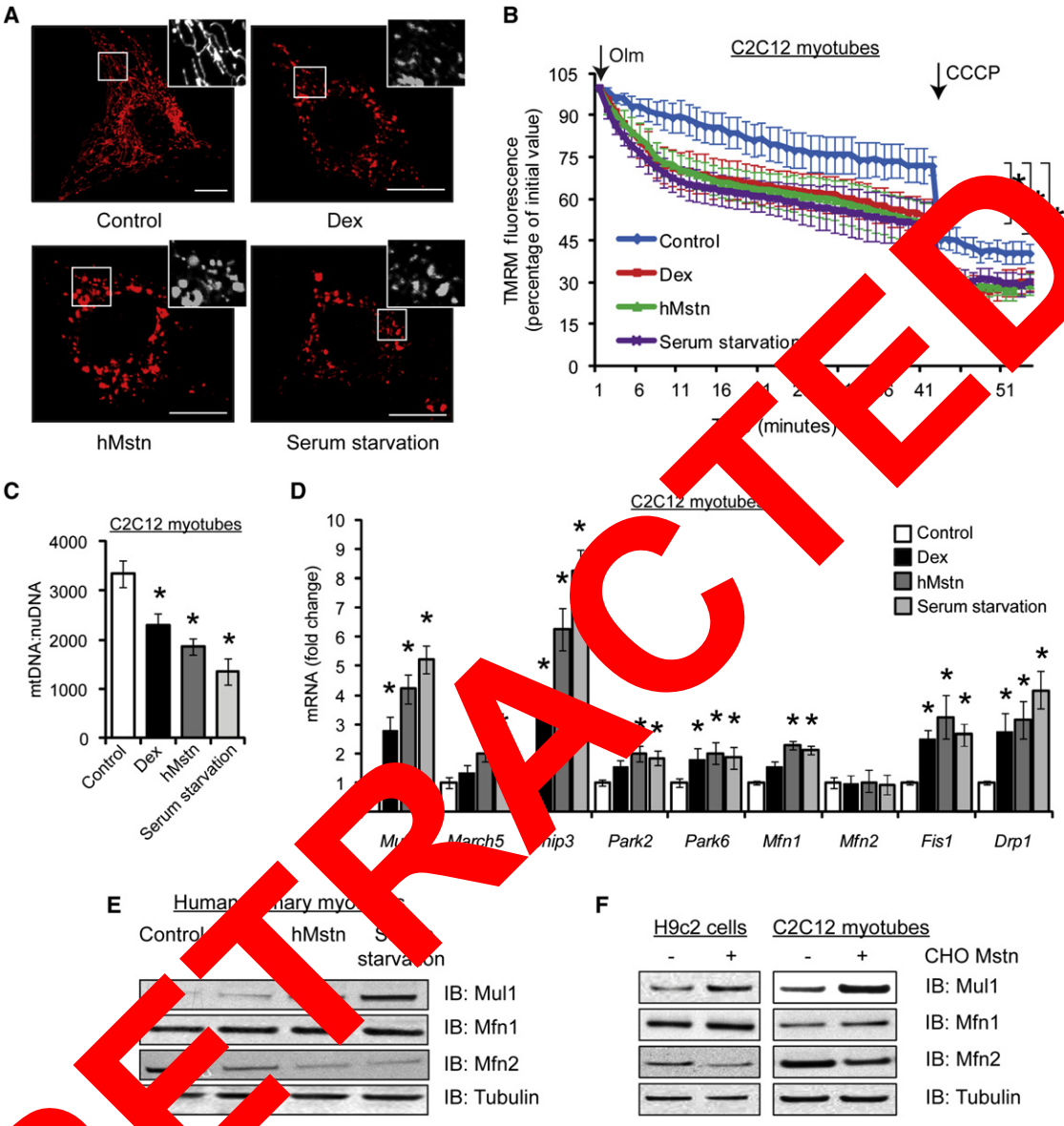


**Figure 1. Dexamethasone, Myostatin, and Serum Starvation Induced Mitochondrial Dysfunction and Promoted Mul1 Expression In Vitro**

(A) Visualization of mitochondria in C2C12 myoblasts following 24 hr treatment with Dexamethasone (Dex) and recombinant human Myostatin protein (hMstn) and during serum starvation. Mitochondria were visualized by mtRed fluorescence. Scale bars represent 10 μm.

(B) Quantitative analysis of the change in tetramethylrhodamine, methyl ester (TMRM) fluorescence in mitochondria from C2C12 myotubes. Cells were treated with Dex and hMstn and subjected to serum starvation for 24 hr before TMRM loading. Arrows indicate when 5 μM of oligomycin (Olm) and 5 μM of protonophore Carbonyl cyanide chlorophenylhydrazone (CCCP) were added. Statistical significance was assessed between control and treatment groups after Olm treatment and before addition of CCCP. Values are means ± SD; n = 8. *$p < 0.01$.

(C) Quantitative analysis of the ratio of mtDNA copy number to nuDNA (mtDNA:nuDNA) following treatment with Dex and hMstn and during serum starvation in C2C12 myotubes. Values are means ± SD; n = 5. *$p < 0.01$.

(D) RT-qPCR analysis of mitochondrial gene expression in C2C12 myotubes treated with Dex and hMstn and during serum starvation for 24 hr. Gene expression was normalized to three endogenous controls, *Gapdh*, *Actb*, and *Gusb*, using the ΔΔCT method. Values are means ± SD; n = 6. *$p < 0.01$.

(E) Immunoblot (IB) analysis of Mul1, Mfn1, and Mfn2 protein expression in human primary myotubes (hMb15) treated with Dex and hMstn and during serum starvation.

(F) IB analysis of Mul1, Mfn1, and Mfn2 protein expression in H9c2 rat cardiomyocytes and C2C12 myotubes after 24 hr treatment with (+) or without (–) eukaryotically produced Mstn protein (CHO Mstn) (see also Figure S1).

Endogenous FoxO1 and FoxO3 expression in C2C12 myotubes was also silenced by siRNA to delineate the specificity of the FoxO transcription factors in regulating the expression of Mul1 during serum starvation and treatment with Dex or hMstn (Figure 2B and Figure S2B). Results demonstrated that the knockdown of FoxO1 and FoxO3 led to a reduction in Mul1

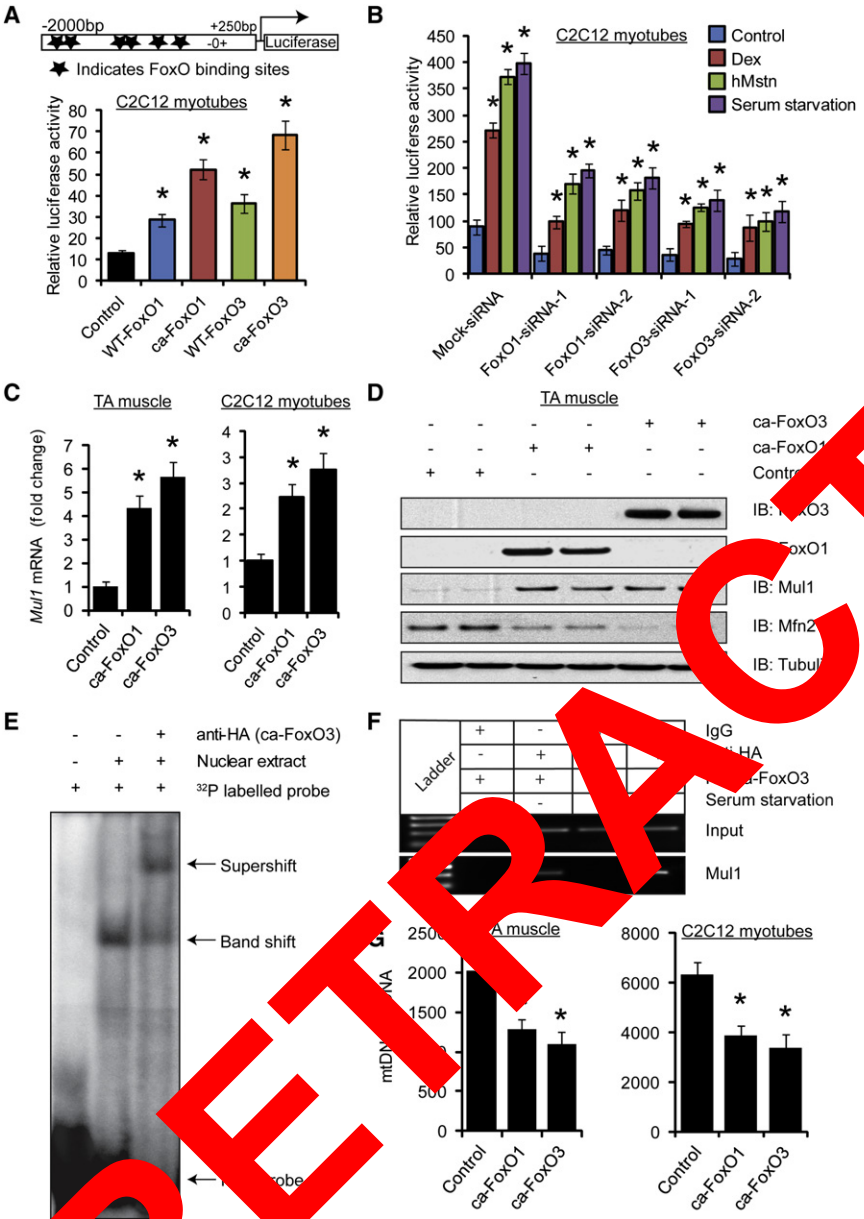


**Figure 2. FoxO Transcription Factors Regulate Mul1 Expression**

(A) Schematic representation of the human Mul1 (hMul1) promoter-reporter construct used in subsequent luciferase assays (Top). Consensus FoxO binding sites (RTAAAYA), as determined by in silico analysis, are represented by stars. (Bottom) Analysis of hMul1 promoter-reporter activity in 72 hr differentiated C2C12 myotubes transfected with hMul1 reporter construct with WT-FoxO1, ca-FoxO1, WT-FoxO3, or ca-FoxO3. All values are normalized to renilla luciferase and are compared to empty vector control (Control). Data represent mean ± SD; n = 8; *p < 0.01.

(B) Analysis of Mul1 promoter reporter luciferase activity in FoxO1 and FoxO3 knockdown C2C12 myotubes differentiated for 72 hr and treated with Dex or hMstn and response to serum starvation for 24 hr. Values are normalized to renilla luciferase activity and are compared to empty vector control (Control). Data represent mean ± SD; *p < 0.01.

(C) qPCR analysis of *Mul1* expression in TA muscle (left) and C2C12 myotubes (right) transfected with ca-FoxO1, ca-FoxO3, or empty vector control (Control). Gene expression was normalized to the endogenous control, *Gapdh*, using the ΔΔCT method. Values are means ± SD; n = 6. *p < 0.01.

(D) IB analysis of Mul1, FoxO3, FoxO1, and Mfn2 protein levels in TA muscle transfected with ca-FoxO1, ca-FoxO3, or empty vector control (Control).

(E) Electrophoretic mobility shift assay (EMSA) on nuclear extracts from 293T cells transiently transfected with HA-ca-FoxO3 and a double-stranded $^{32}$P-labeled oligonucleotide probe containing hMul1 FoxO binding sites (−1,220 bp and −1,204 bp). A band shift was noted after the addition of nuclear extract and a supershift upon addition of anti-HA antibody, confirming interaction of HA-ca-FoxO3 with the probe.

(F) To assess for interaction between FoxO3 and Mul1, chromatin immunoprecipitation (ChIP) was performed in C2C12 myotubes stably transfected with HA-ca-FoxO3. Cultures were either grown under control conditions (−) or subjected to 24 hr of serum starvation (+).

(G) Analysis of mtDNA:nuDNA ratio in M. *tibialis anterior* (TA) muscle (left) and C2C12 myotubes (right) transfected with ca-FoxO1, ca-FoxO3, or empty vector control (Control). Values are means ± SD; n = 5. *p < 0.01 (see also Figure S2).



promoter-reporter-driven luciferase activity during serum starvation and treatment with Dex or hMstn, when compared to scrambled siRNA (Mock-siRNA) transfected controls (Figure 2B).

Knockdown of FoxO1 and FoxO3 also resulted in the reduction of Mul1 protein levels and an increase in Mfn2 protein expression (Figure S2B). Moreover, transfection of ca-FoxO1 or ca-FoxO3 into TA muscle led to increased Mul1 mRNA and protein expression (Figures 2C and 2D). Similarly elevated Mul1 mRNA and protein expression was observed in C2C12 myotubes expressing ca-FoxO1 or ca-FoxO3 (Figure 2C and Figure S2A). Importantly, we found significantly reduced Mfn2 protein levels in both ca-FoxO1- and ca-FoxO3-transfected TA muscle and myotubes (Figure 2D and Figure S2A). Furthermore, a significant reduction in mtDNA:nuDNA ratio was observed in C2C12 myoblasts and myotubes and in TA muscle following transfection of either ca-FoxO1 or ca-FoxO3 (Figure 2G and Figure S2C). In agreement, knockdown of FoxO1 or FoxO3 by siRNA significantly rescued the reduced mtDNA:nuDNA ratio observed in C2C12 myotubes during serum starvation and treatment with Dex or hMstn (Figure S2D).

To validate interaction of FoxO transcription factors with the Mul1 promoter, electrophoretic mobility shift assay (EMSA) was performed, using a nuclear extract from HA tagged ca-FoxO3-transfected 293T cells and a probe containing FoxO binding sites from the Mul1 promoter. A strong band shift was

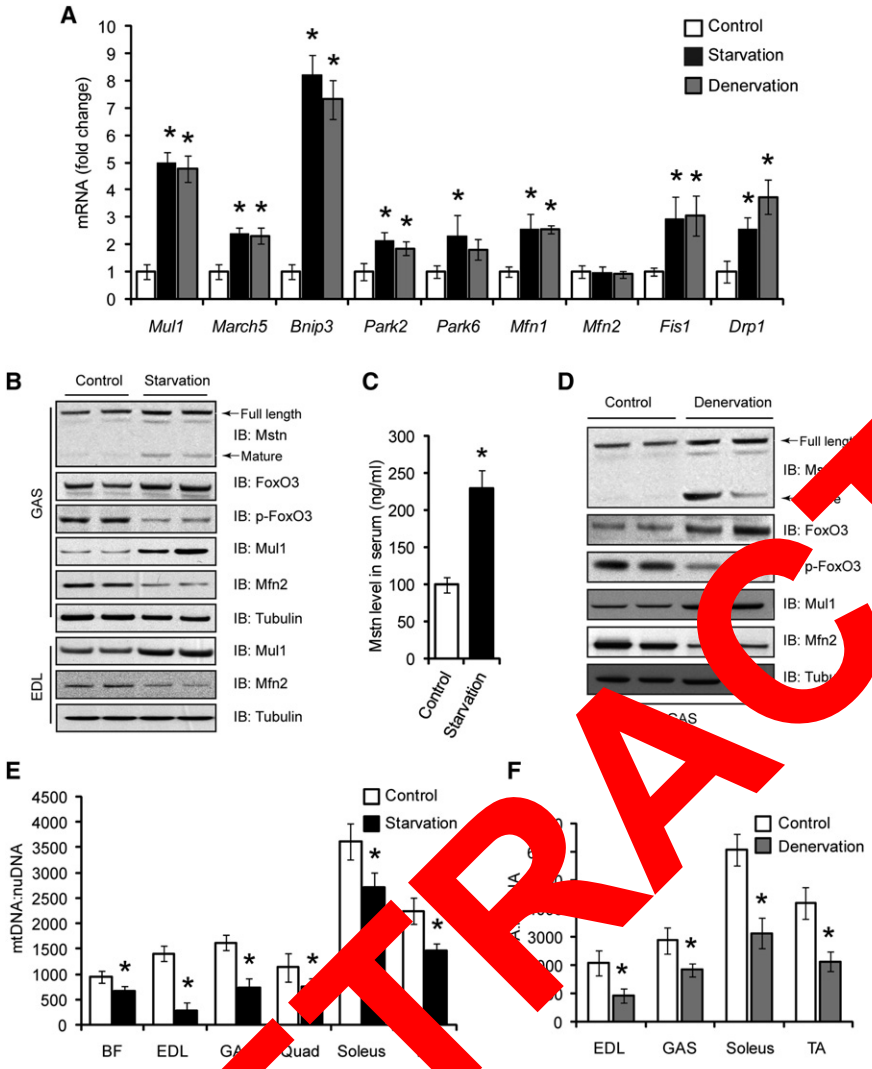


**Figure 3. Starvation and Denervation Promoted the Expression of Mul1 and Reduced mtDNA:nuDNA Ratio In Vivo**

(A) RT-qPCR analysis of mitochondrial gene expression changes in M. *gastrocnemius* (GAS) muscle isolated from starved and denervated mice. Gene expression was normalized to three endogenous controls, G… *Actb*, and *Gusb*, using the ΔΔCT meth… means ± SD; n = 5. *p < 0.01.

(B) IB analysis … n, FoxO3, p-… 3, Mul1, and Mfn2 p…tein l… in GAS mu… isolated from con… and starv… ice (to… B analysis of Mu… d Mfn2 protei… M. *extensor digitorum longus* (EDL) m… isolated from co… nd …ed mice (bottom).

(C) Q… ve asses… t of Mstn levels in serum iso… from … starved for 48 hr. Values are means ± … . *p < 0.01.

(D) IB analysis … Mstn, FoxO3, p-FoxO3, Mul1, … Mfn2 protein levels in GAS muscle isolated fr… ntrol and denervated mice.

(E) A…sis of mtDNA:nuDNA ratio in M. *bicep femoris* (BF), EDL, GAS, M. *quadriceps* (QUAD), soleus, and TA muscles isolated from control and starved mice. Values are means ± SD; n = 5. *p < 0.01.

(F) Analysis of mtDNA:nuDNA ratio in EDL, GAS, soleus, and TA muscles isolated from control and denervated mice. Values are means ± SD; n = 5. *p < 0.01.



observed upon inc… ion … e γ-ATP-[$^{32}$P]-labeled probe with the ca-FoxO3 expres… uclear e…act (Figure 2E). Additionally, a su… was …erv… upon addition of anti-HA antibod… dica… that H… FoxO3 was bound to the Mul1 prom… (Figu… 2E). Chromatin immunoprecipitation (ChIP) verifie… t… interacted with the Mul1 promoter and that … binding of HA-ca-FoxO3 to the Mul1 promoter increased fu… upon serum starvation in C2C12 myotubes (Figure 2F).

## Starvation and Denervation Enhanced Mul1 Levels and Depleted mtDNA:nuDNA Ratio In Vivo

Similar to the in vitro skeletal-muscle-wasting models, elevated *Mul1* expression was detected in M. *gastrocnemius* (GAS) muscles from both starved and denervated mice when compared to controls (Figure 3A). Additionally, the mRNA expression profile of other mitochondrial genes was also comparable to the in vitro muscle-wasting models (compare Figure 1D with Figure 3A). Immunoblot analysis confirmed elevated Mul1 protein levels in GAS and M. *extensor digitorum longus* (EDL) muscles during starvation and in GAS muscle during denervation (Figures 3B and 3D). Furthermore, elevated Mstn and reduced phosphorylated FoxO3 (p-FoxO3) protein levels were observed in muscle tissue isolated from starved and denervated mouse models when compared to respective controls (Figures 3B and 3D). Circulatory levels of Mstn were also elevated in starved mice (Figure 3C). During starvation and denervation, we observed reduced Mfn2 protein levels in skeletal muscles (Figures 3B and 3D). However, *Mfn2* mRNA expression was unchanged in GAS muscles collected from both starved and denervated mice when compared to control (Figure 3A). Importantly, mtDNA:nuDNA ratio was also significantly reduced in numerous skeletal muscle tissues isolated from starved and denervated mice (Figures 3E and 3F).

## Mul1 Ubiquitinated and Targeted Mfn2 for Degradation

To verify whether Mul1 directly facilitates the degradation of Mfn2 through the ubiquitin-proteasome system, we induced Mul1 expression in C2C12 myotubes by serum starvation and examined the protein levels of Mfn2 in the presence or absence of the proteasome inhibitor, MG132. Immunoblot analysis demonstrated that serum starvation-induced loss of Mfn2 protein in C2C12 myotubes was prevented through MG132-mediated blockade of the proteasome, despite sustained upregulation of Mul1 (Figure 4A). Furthermore, proteasome inhibition also prevented a reduction in mtDNA:nuDNA ratio in serum-starved myotubes (Figure S3A).

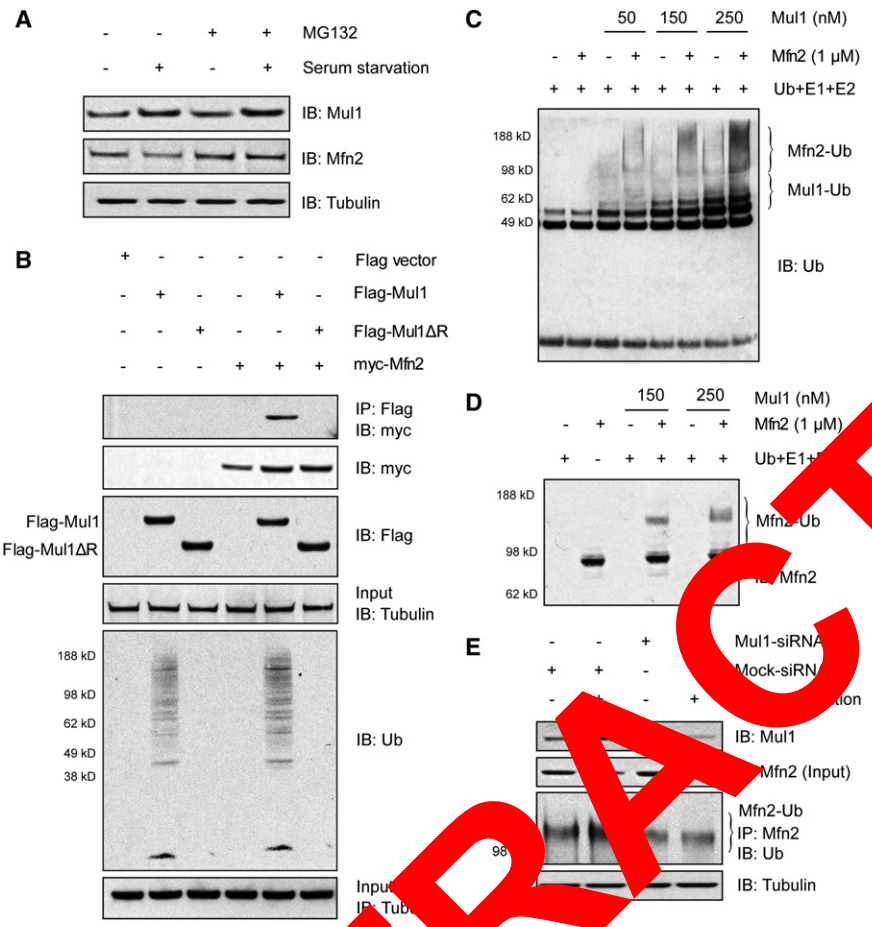


**Figure 4. Mul1 Ubiquitinated and Targeted Mfn2 for Degradation through the Ubiquitin-Proteasome Pathway**

(A) IB analysis of Mul1 and Mfn2 protein levels in control (−) and 24 hr serum-starved (+) myotube cultures in the absence (−) or presence (+) of the proteasome inhibitor MG132.

(B) Coimmunoprecipit[illegible]/Co-IP) analysis of C2C12 myoblasts [illegible]ith Flag-tagged Mul1 (Flag-Mul[illegible]d myc-ta[illegible] Mfn2 (myc-Mfn2) construc[illegible]teraction bet[illegible]n Mul1 and Mfn2 was verifie[illegible]ough the [illegible]sfection of a RING[illegible]ger dele[illegible] Mul1 [illegible]struct (Flag-Mul[illegible]. IB analysis o[illegible]inated proteins c[illegible]munopr[illegible]ated with[illegible]g-Mul1 (bottom).

([illegible]l1 [illegible]itinated Mfn2 in vitro. Myc-DDK-hM[illegible]; full leng[illegible] μM) was incubated with yeast [illegible] (E1) ([illegible]M), hUbcH5c (E2) (4 μM), $His_6$-biotin[illegible]ub) (5 μM), and increasing concentration[illegible]f GST-hMul1 (Mul1; full length) [illegible]0, 150, and 250 nM) for 1 hr. IB analysis with an [illegible]ubiquitin antibody (Ub) is shown, and the ub[illegible]inated Mfn2 protein (Mfn2-Ub) is indicated within the brackets.

(D) To confirm Mul1 ubiquitin ligase activity on Mfn2, myc-DDK-hMfn2 (Mfn2; full length) (1 μM) was incubated with yeast UBE1 (E1) (125 nM), hUbcH5c (E2) (4 μM), $His_6$-biotin-hUB (Ub) (5 μM), and increasing concentrations of GST-hMul1 (Mul1; full length) (150 and 250 nM) for 1 hr. IB analysis with anti-Mfn2 is displayed, and band shifts indicate polyubiquitinated Mfn2.

(E) IB analysis with anti-Ub antibody on the Mfn2-immunoprecipitated complex collected from Mul1-silenced (Mul1-siRNA) and scrambled siRNA (Mock-siRNA)-transfected serum-starved and control C2C12 myotubes. Ubiquitinated Mfn2 protein (Mfn2-Ub) is indicated within the brackets. IB analysis of Mul1 and Mfn2 inputs are shown (see also Figure S3).



To confirm whet[illegible] Mul1 associate[illegible]ith Mfn2, C2C12 myoblasts were c[illegible]ansfect[illegible]with either Flag-Mul1 or a Flag-Mul1 deletion c[illegible]uct[illegible]here the RING finger domain has been deleted (Fla[illegible]1ΔR), t[illegible]ther with the myc-Mfn2 expressi[illegible]truct. [illegible]Mu[illegible]rotein complex was immunoprecip[illegible]ed us[illegible] anti-F[illegible]ubodies and analyzed for coimmu[illegible]recipit[illegible]n of myc-Mfn2. Immunoblot analysis revealed that [illegible]cipitated with Mul1, suggesting that Mul1 as[illegible]tes with Mfn2 (Figure 4B). Coimmunoprecipitation experiment[illegible]so identified that the RING finger domain of Mul1 is requir[illegible]or this interaction, as Mul1 did not coimmunoprecipitate with Mfn2 in myoblasts cotransfected with Flag-Mul1ΔR and myc-Mfn2 (Figure 4B).

An immunoblot with anti-ubiquitin antibody on the Flag-Mul1 coimmunoprecipitated complex further demonstrated the presence of several ubiquitinated proteins, indicating the ubiquitin ligase activity conferred by Mul1 (Figure 4B). To determine whether Mul1 directly ubiquitinated Mfn2, we performed an in vitro ubiquitination assay. Incubation with increasing concentration of Mul1 resulted in increased levels of ubiquitinated Mfn2 (Figures 4C and 4D). Ubiquitinated Mfn2 bands were detected above the molecular weight of nonubiquitinated Mfn2 (Figures 4C and 4D). To confirm whether Mul1 ubiquitinated Mfn2 in muscle cell cultures, Mul1 expression in C2C12 myotubes was silenced by siRNA, and protein lysates were immunoprecipated with anti-Mfn2 antibodies. Subsequent anti-Ub immunoblot analysis of the Mfn2 immunoprecipitated lysates revealed reduced amounts of ubiquitinated Mfn2 in Mul1-silenced C2C12 myotubes, when compared to scrambled siRNA controls (Mock-siRNA) (Figure 4E).

In addition to ubiquitinated Mfn2, we also detected ubiquitinated Mul1 (Figure 4C). We suggest that Mul1 ubiquitination was due to Mul1 autoubiquitination, since incubation of increasing concentrations of Mul1 with E1, E2, and Ub correlated in a dose-dependent manner with increased levels of ubiquitinated Mul1 (Figure S3B).

## Mul1 Overexpression Facilitated Mitochondrial Dysfunction and Skeletal Muscle Atrophy

To further characterize Mul1 function, we cotransfected C2C12 myoblasts with Mul1 overexpression vector (GFP-Mul1) and mtRed and examined mitochondria morphology. Confocal imaging revealed that overexpression of Mul1 promoted mitochondrial fragmentation in C2C12 myoblasts (Figure 5A). Furthermore, transfection of GFP-Mul1 into C2C12 myoblasts resulted in significantly increased mitochondrial depolarization

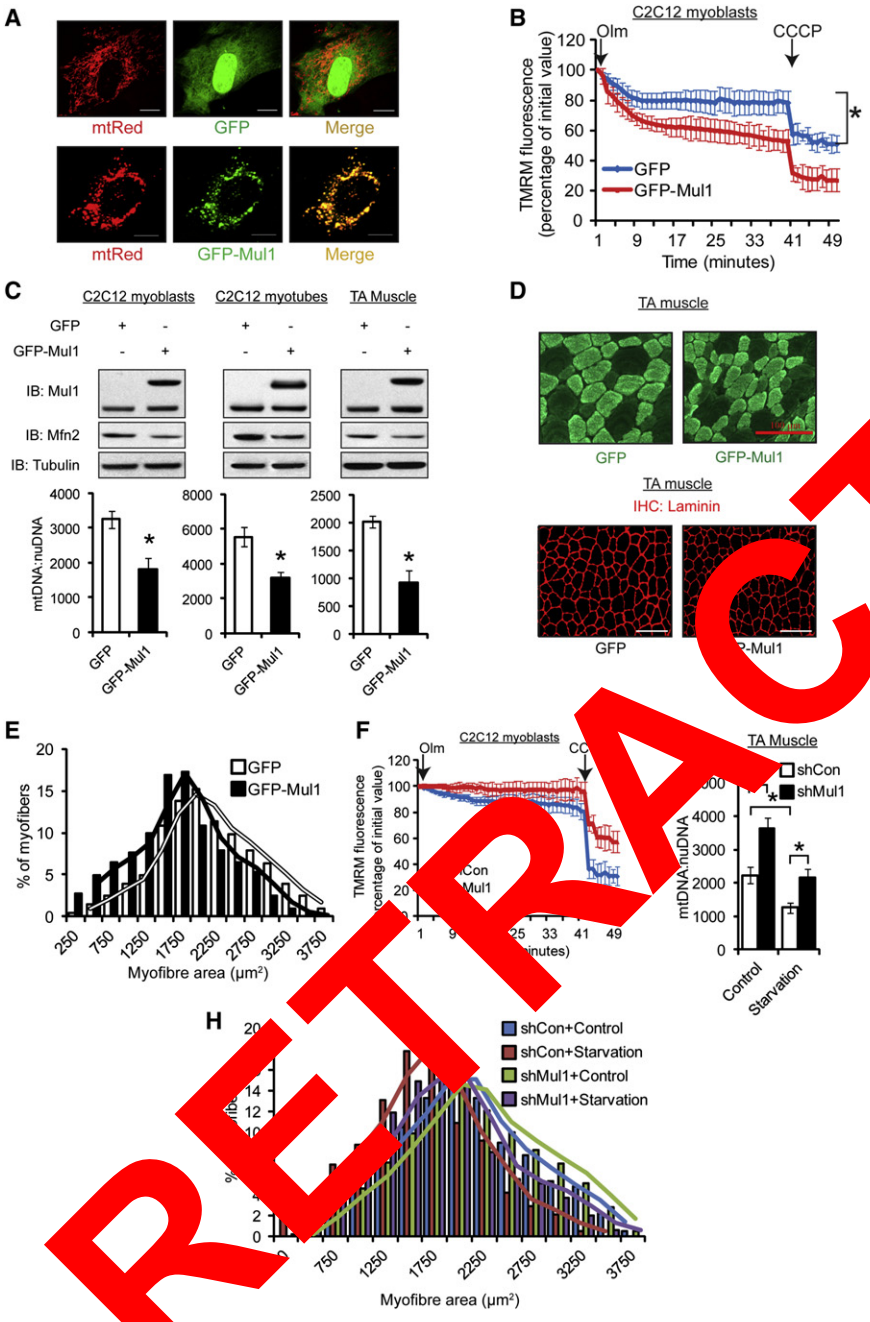




**Figure 5. Mul1 Facilitated Mitochondrial Dysfunction**

(A) Visualization of mitochondria following overexpression of a GFP-tagged Mul1 construct (GFP-Mul1) and empty GFP vector (GFP) in C2C12 myoblasts. Mitochondria were visualized by mtRed fluorescence. Scale bars represent 10 μm.

(B) Quantitative analysis of TMRM fluorescence changes over mitochondria in C2C12 myoblasts transfected with either control (GFP) or GFP-Mul1. Arrows indicate when 5 μM of Olm and 5 μM CCCP were added. Statistical significance was assessed between GFP- and GFP-Mul1-transfected C2C12 myotubes after Olm treatment and before addition of CCCP. Values are means ± SD; n = 3. *p < 0.01.

(C) Analysis of mtDNA:nuDNA ratio in C2C12 myoblasts (left), myotubes (middle), and TA muscle (right) transfected with either empty GFP vector (GFP) or GFP-Mul1 (right). Values are means ± SD; n = 5. *p < 0.01. IB analysis of Mul1 and Mfn2 in myoblasts, myotubes, and TA muscles is also displayed.

(D) Representative microscopy images of TA muscle sections 9 days after GFP and GFP-Mul1 overexpression vector transfection (top). Scale bars represent 100 μm. Laminin staining on GFP- and GFP-Mul1-transfected TA muscle (bottom). Scale bars represent 50 μm. Muscles were collected 9 days posttransfection. The contralateral limb TA muscle was transfected with the control GFP vector.

(E) Frequency distribution (%) of myofiber area ($\mu m^2$) in TA muscle cryosections 9 days posttransfection with either GFP or GFP-Mul1 overexpression vector. The contralateral limb TA muscle was transfected with the control GFP vector. Four hundred myofibers from three sections per group were analyzed using the ImagePro Plus software.

(F) Quantitative analysis of TMRM fluorescence changes in mitochondria from C2C12 myoblasts transfected with either control nonsilencing shRNA (shCon) or Mul1 shRNA (shMul1). Arrows indicate when 5 μM of Olm and 5 μM CCCP were added. Statistical significance was assessed between shCon- and shMul1-transfected C2C12 myotubes after Olm treatment and before addition of CCCP. Values are means ± SD; n = 8. *p < 0.01.

(G) Analysis of mtDNA:nuDNA ratio in TA muscle isolated from control or 48 hr starved mice 9 days after transfection with either shCon or shMul1. Values are means ± SD; n = 5. *p < 0.01.

(H) Frequency distribution (%) of myofiber area ($\mu m^2$) in TA muscle cryosections 9 days posttransfection with either shCon or shMul1 and following an additional period of 48 hr starvation. The contralateral limb TA muscle was transfected with shCon. Four hundred myofibers from three sections per group were analyzed using the ImagePro Plus software. (See also Figure S4.)

when compared to the GFP empty vector-transfected control after Olm treatment (Figure 5B). Ectopic expression of Mul1 in C2C12 myoblasts and myotubes and in TA muscle also resulted in significantly reduced mtDNA:nuDNA ratio (Figure 5C). Furthermore, overexpression of Mul1 in TA muscle led to reduced myofiber area and muscle weight when compared to controls (Figures 5D and 5E and Figure S4A).

When Mul1-specific siRNA (Mul1-siRNA) was transfected into C2C12 myoblasts, we observed an expansive and elongated mitochondrial network (visualized by mtRed), which was qualitatively greater than the mitochondrial network in the scrambled siRNA (Mock-siRNA)-transfected control (Figure S4B). Knockdown of Mul1 in C2C12 myoblasts also appeared to confer resistance to mitochondrial fragmentation induced by Dex and hMstn and in response to serum starvation (Figure S4B) and prevented mitochondrial depolarization even after treatment with Olm (Figure 5F). We also observed a stark increase in mtDNA:nuDNA ratio in shMul1-transfected

TA muscle when compared to the control shRNA (shCon) transfected contralateral TA muscle (Figure 5G). Moreover, we observed a rescue of mtDNA:nuDNA ratio in the shMul1-transfected TA muscle of starved mice undergoing muscle wasting, when compared to shCon-transfected starved mice, back to levels comparable to shCon-transfected control mice (Figure 5G). Additionally, Mul1 silencing in C2C12 myotubes blocked the reduction in mtDNA:nuDNA ratio observed following treatment with Dex or hMstn or during serum starvation, enhanced the protein levels of Mfn2, and further prevented hMstn-mediated degradation of Mfn2 (Figures S4C and S4D). In support, knockdown of Mul1 in TA muscle partially rescued the reduced myofiber area and muscle weight observed during starvation when compared to control (shCon)-transfected TA muscles (Figure 5H, Figures S4E and S4F). Furthermore, elevated amounts of Mfn2 protein were observed in both shMul1-transfected TA muscles of starved and control mice when compared to respective shCon-transfected contralateral TA muscles (Figure S4G).

## Mul1 Overexpression Induced Mitophagy

Significant reduction in mitochondrial copy number is associated with mitophagy, the selective degradation of mitochondria through the autophagy-lysosomal pathway (Youle and Narendra, 2011). Consistent with enhanced mitopha noted increased autophagosome formation and enhanced vels of LC3-II in C2C12 cultures exposed to Dex and hMstn a in response to serum starvation (Figures S5A and S5B). He we surmised that Mul1 overexpression stim Dex a hMstn and in response to serum star n mic serve a a potent signal for mitophagy. Indeed, C2 blasts were treated with Dex or hMstn or n u um sta ion conditions, we noted colocali n of mito ndria, demarcated by mtRed, with GF positive au agosomes, which is indicative of mitop gy (Fig S5C). To fu her quantify mitophagy in muscle c res, we ect lly expressed a lysosomal protease-res nt coral prote MT-mKeima-Red, which localizes to matri the mitochondria (Kogure et al., 2006), in C2C12 ube ior to serum starvation or treatment with Dex or hMstn -mKeim ed exhibits a bimodal excitation p n at 4 d 5 m that occurs when the mitochond targe protei ound in a neutral or acidic pH, res ively. quantifying the 586/440 nm excitation ratio, the p eima-Red-tagged mitochondria fused to lysos s can be ascertained. Serum-starved, Dex- and hMstn-trea pMT-mKeima-Red-expressing C2C12 myotubes demonstrated high 585/440 nm ratio when compared to control, confirming that a large population of mitochondria in the C2C12 myotubes were fused to lysosomes in response to catabolic stimuli (Figure 6A). Furthermore, pMT-mKeima-Red-expressing myotubes treated with Olm and CCCP, two potent inducers of mitophagy, demonstrated the greatest degree of mitophagy as the 586/440 nm ratio was the highest across all the treatments (Figure 6A).

GFP-Mul1 tagged mitochondria colocalized with RFP-LC3-positive autophagosomes in C2C12 myoblasts 24 hr after transfection of GFP-Mul1 overexpression plasmid (Figure 6B). To confirm whether Mul1 overexpression promoted mitophagy, we ectopically expressed pMT-mKeima-Red in GFP-Mul1-transfected C2C12 myotubes and measured the 585/440 nm ratio. GFP-Mul1-expressing myotubes exhibited a higher 585/440 nm ratio compared to the GFP control C2C12 myotubes, further supporting Mul1 as an inducer of mitophagy (Figure 6C). GFP-Mul1 overexpression in C2C12 myotubes and in TA muscle also resulted in increased levels of LC3-II (Figure 6D). However, knockdown of Mul1 impeded increased LC3-II levels observed in C2C12 myotube cate th Dex and hMstn and during serum starvati (Figure S A similar reduction in LC3-II levels was also rved upon ockdown of Mul1 in TA muscle of sta d mic ure 6E onsistent with the above results, 2 protein e markedly reduced in both C2C1 yotub and T uscles overexpressing GFP-Mul1 ( Conversely, knockdown of Mul1 in C2C12 otube d TA cle increased Mfn2 protein levels ite conti nce of Dex, hMstn, or starvation s hen compa o respective controls (Figure S5D a Figu F). Furthermore, knockdown of Mul1 in serum-starved, Dex hMstn-treated pMT-mKeima-Red-tra d C2C12 myo es led to a low 585/440 nm ratio w n compared to respective scrambled siRNA-transfected c trols, furth confirming that Mul1 knockdown prevented m hagy in tube cultures exposed to catabolic stimuli (Fig 6F).

## Mul1 Was Weakly Expressed in Slow-Twitch Muscles and Differentiated Myotubes

Although we have demonstrated that increased expression of Mul1 imparts pathological consequences during skeletal muscle wasting, the normal physiological role of Mul1 in skeletal muscle remains unclear. Hence, we next quantified the expression of Mul1 in fast- and slow-twitch muscles. Interestingly, the predominantly slow-twitch (type I) soleus muscle displayed reduced amounts of Mul1 together with lower levels of Mstn, when compared to the predominantly fast-twitch (type IIa/b/x) TA muscle (Figure 7A). Consistent with this, Mfn2 protein level and mtDNA:nuDNA ratio was higher in soleus muscle when compared to TA muscle (Figure 7B).

We further noted temporal variation in Mul1 expression during myogenesis (Figure 7C). Specifically, Mul1 protein levels were less in differentiated C2C12 myotubes when compared to proliferating C2C12 myoblasts (Figure 7C). In addition, reduced Mul1 levels in myotubes were associated with decreased Mstn protein and a reciprocal increase in Mfn2 abundance (Figure 7C). In agreement, the mtDNA:nuDNA ratio was also increased in myotubes when compared to myoblasts (Figure 7D).

## DISCUSSION

Mitochondrial dysfunction underlies various human pathologies, including adult-onset neurodegeneration, cancer, aging, cardiovascular disease, and metabolic disorders, such as obesity and type 2 diabetes (Dodson et al., 2011; Emery, 2002; Evans, 2010; Lecker, 2003). Autophagy-lysosome-mediated removal of malfunctioning mitochondria in the skeletal muscles of fasted and denervated mice was recently documented to result in exacerbated skeletal muscle wasting (Romanello et al., 2010). However, to date, the exact mechanism that results in

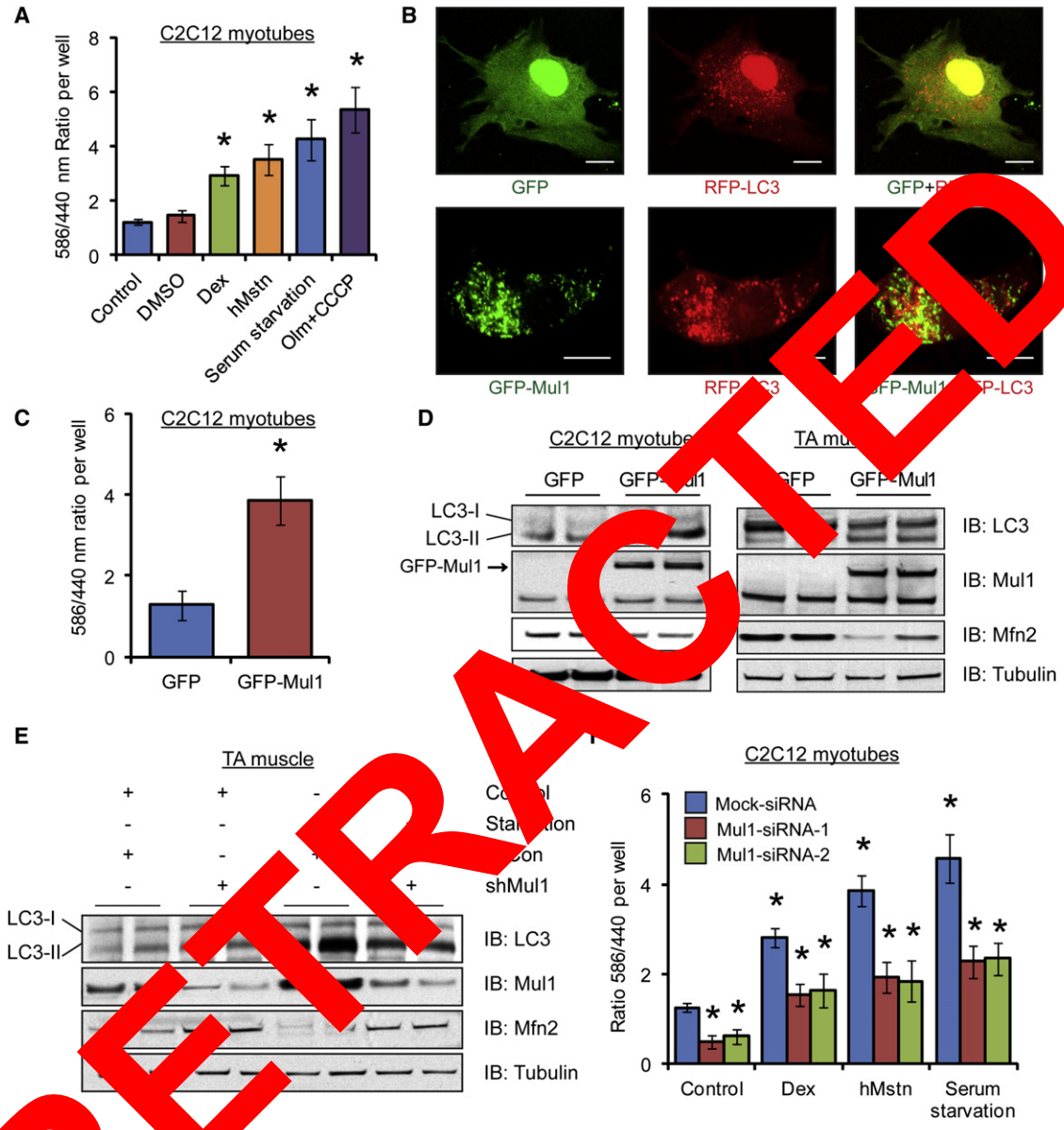


**Figure [illegible] Mul1 Overexpression Induced Mitophagy**

(A) Exc[illegible] rati[illegible] of pMT-mKeima-Red expressing C2C12 myoblasts following serum starvation, Dex treatment, or hMstn treatment, where a high 586/440 n[illegible] indicative of increased mitophagy. Positive controls for the induction of mitophagy (Olm and CCCP) are also shown. Values are means ± SD; n = 32. *p < 0[illegible]

(B) Visualization [illegible]FP-Mul1 and RFP-LC3-positive autophagosomes in GFP-Mul1 and RFP-LC3 cotransfected C2C12 myoblasts. C2C12 myoblasts transfected with the GF[illegible]mpty vector (GFP) and RFP-LC3 are displayed. Scale bars represent 10 μm.

(C) Excitation ratio (586/440 nm) of pMT-mKeima-Red-expressing C2C12 myoblasts cotransfected with either control (GFP) or GFP-Mul1 constructs. A high 586/440 nm ratio is indicative of mitophagy. Values are means ± SD; n = 32. *p < 0.01.

(D) IB analysis of unlipidated (LC3-I) and lipidated (LC3-II) LC3, Mul1, and Mfn2 protein levels in C2C12 myotubes (left) or TA muscle (right) transfected with either control (GFP) or GFP-Mul1 overexpression constructs.

(E) IB analysis of unlipidated (LC3-I) and lipidated (LC3-II) LC3, Mul1, and Mfn2 protein levels in TA muscle from control or 48 hr starved mice 9 days after transfection with either shCon or shMul1. The contralateral limb TA muscle was transfected with shCon.

(F) Excitation ratio (586/440 nm) of pMT-mKeima-Red in serum-starved, Dex- or hMstn treated C2C12 myotubes expressing either scrambled control siRNA (Mock-siRNA) or Mul1-siRNA (Mul1-siRNA-1 and Mul-siRNA-2). A high 586/440 nm ratio is indicative of mitophagy. Values are means ± SD; n = 32. *p < 0.01 (see also Figure S5).

mitochondria malfunction is not well defined. Here we show that various muscle wasting signals, such as Dex, Mstn, starvation, and denervation, not only disrupt mitochondrial function but also promote mitophagy, the loss of mitochondria through the autophagy-lysosomal system, via upregulation of the mitochondrial E3 ligase Mul1 (Figure S6).

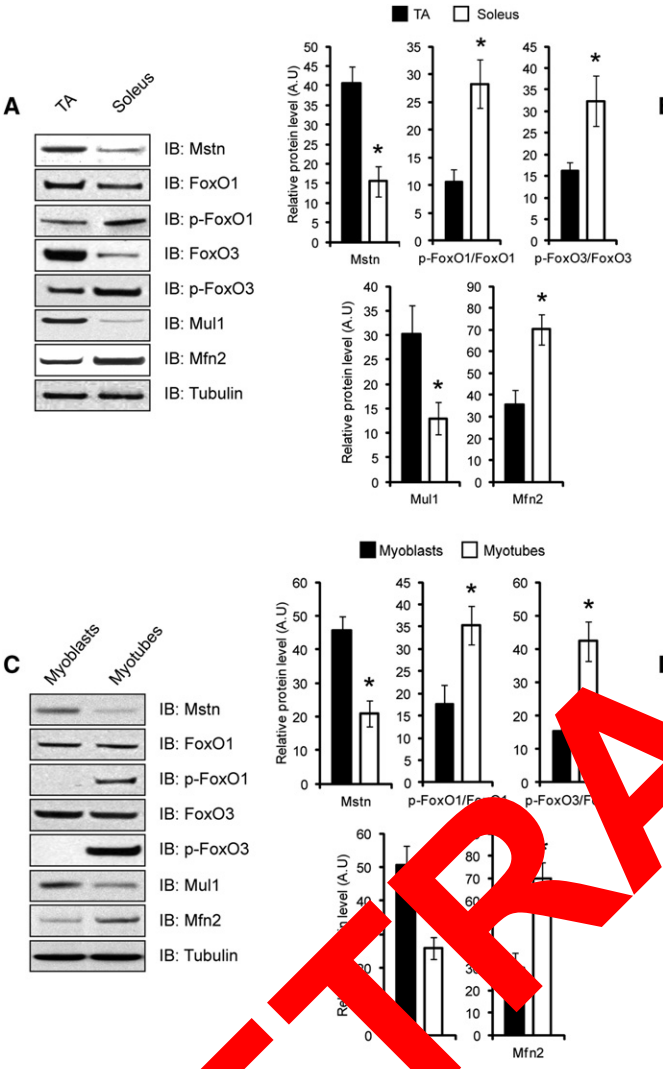


**Figure 7. Mul1 Was Weakly Expressed in Slow-Twitch Muscles and in Myotube Cultures**

(A) IB analysis of Mstn, FoxO1, p-FoxO1, FoxO3, p-FoxO3, Mul1, and Mfn2 protein levels in soleus and TA muscles isolated from wild-type mice (left). (Right) Densitometric analysis of IB showing relative protein levels for Mstn, p-FoxO1/FoxO1, p-FoxO3/FoxO3, Mul1, and Mfn2 normalized to Tubulin. Values are means ± SD; n = 4. *p < 0.01.

(B) Analysis of mtDNA:nuDNA ratio in soleus and TA muscles isolated from wild-type mice. Values are means ± SD; n = 4. *p < 0.01.

(C) IB analysis of Mstn, FoxO1, p-FoxO1, FoxO3, p-FoxO3, Mul1, and Mfn2 protein levels in both proliferating C2C12 myoblasts and 96 hr differentiated C2C12 myotube cultures (left). (Right) Densitometric analysis of IB showing relative protein levels for Mstn, p-FoxO1/FoxO1, p-FoxO3/FoxO3, Mul1, and Mfn2 normalized to Tubulin. Values are means ± SD; n = 4. *p < 0.01.

(D) Analysis of mtDNA:nuDNA ratio in proliferating C2C12 myoblasts and in 96 hr differentiated C2C12 myotubes. Values are means ± SD; n = 4. *p < 0.01.



The mitochondrial E3 ligase, Mul1, is an outer mitochondrial membrane protein that possesses two transmembrane domains and a C-terminal RING finger domain and functions to regulate the fusion and fission of mitochondria (Braschi et al., 2009; Li et al., 2008; Zhang et al., 2008). Since we observed dramatic upregulation of Mul1 in both muscle cell cultures and skeletal muscle exposed to muscle-wasting stimuli, we surmised that this mitochondrial E3 ligase might be responsible for mitochondrial dysfunction and loss associated with muscle wasting. Indeed, ectopic overexpression of Mul1 promoted fragmentation, depolarization, and removal of mitochondria through mitophagy. Furthermore, knockdown of Mul1 expression in C2C12 myoblasts led to an expansive and fused network of healthy mitochondria and further prevented mitochondrial fragmentation, depolarization, and mitophagy induced in response to muscle-wasting signals, suggesting that Mul1 is required for the mitochondrial fission observed in wasting skeletal muscle tissue. In addition, blockade of Mul1 partially rescued myofiber atrophy in the presence of muscle-wasting stimuli, which indicates that Mul1-induced mitochondrial dysfunction has a critical role in the progression of skeletal muscle wasting.

Fragmentation of mitochondria occurs due to stabilization of mitochondrial fission proteins, degradation of mitochondrial fusion proteins, or a combination of both (Chen et al., 2010; Romanello et al., 2010). According to previously published reports, Mul1 has been shown to stabilize Drp1, a mitochondrial fission protein, resulting in mitochondrial fragmentation (Braschi et al., 2009). In this study, we report that Mfn2 is a downstream target of Mul1. Using coIP we clearly show that Mfn2 physically interacts with Mul1 and that the RING finger domain of Mul1 is essential for this interaction. Our results also confirm that Mul1 ubiquitinates and targets Mfn2 for degradation through the ubiquitin-proteasome pathway. Mfn2 is a critical mitochondrial fusion protein; thus we hypothesize that Mul1-mediated removal of Mfn2 through the ubiquitin-proteasome pathway, together with the stabilization of Drp1, could account for the extensive mitochondrial fission observed during skeletal muscle wasting.

FoxO3 is emerging as a master regulator of the skeletal muscle atrophy program. Indeed, FoxO3 activation in response to procachectic stimuli, such as Myostatin or Dexamethasone, results in increased Atrogin-1 and MuRF1 and enhanced activation of the ubiquitin-proteasome system (Lokireddy et al., 2011a; McFarlane et al., 2006; Sandri et al., 2004; Zhao et al., 2007). Furthermore, FoxO3 has also been shown to activate numerous genes involved in the autophagy-lysosome pathway, particularly LC3, Beclin-1, Atg7, Bnip3, Cathepsin L, and Gabarap1 (Mammucari et al., 2007; Romanello et al., 2010; Zhao et al., 2007). In this study we have demonstrated that FoxO3 transcriptionally regulates Mul1 expression during skeletal muscle wasting. Several lines of evidence presented in this study confirm

that Mul1 is transcriptionally regulated by FoxO transcription factors. Initial in silico analysis identified six FoxO binding sites in the 2 kb upstream promoter region of the *Mul1* gene. Furthermore, cotransfection of the Mul1 promoter-reporter construct with constitutively active FoxO1/3 resulted in several-fold induction of Mul1 reporter activity. In addition, both EMSA and ChIP assays confirmed that FoxO3 physically interacts with FoxO binding elements in the Mul1 promoter region, which was enhanced in the presence of muscle-wasting stimuli. Therefore, we propose that enhanced FoxO1/3 activity during muscle wasting results in increased transcription of Mul1, which in turn ubiquitinates and degrades Mfn2, resulting in mitochondrial dysfunction and loss during muscle wasting.

While the majority of this report has focused on understanding the function of Mul1 during skeletal muscle wasting, we were intrigued to observe differential expression of Mul1 between fast- and slow-twitch muscles. Slow-twitch muscle, which is aerobic in nature, had low amounts of Mstn and Mul1 together with increased Mfn2 protein levels and mitochondrial number, whereas in contrast, fast-twitch muscle, which is typically anaerobic, expressed higher levels of Mstn and Mul1, reduced Mfn2, and contained relatively low numbers of mitochondria. Based on these data, we propose that Mul1, through regulating mitochondrial number, plays an integral role in modulating the energy balance of skeletal muscle and thus the ae anaerobic status of muscle fibers.

In conclusion, induction of muscle wasting led to enhan FoxO-mediated activation of Mul1, which further p oted mi chondrial fragmentation, depolarization, and in bot muscle cell cultures and skeletal muscle ti . Take ogether, these data presented in this manuscript rscov r- tance of mitochondrial function in th prog of ske al muscle wasting.

## EXPERIMENTAL PROCEDURES

### Animal Care and Handli

All wild-type mice (C57 ) used w obtained from National University of Singapore Centre for al Re es (NUS CARE), Singapore. All experiments were performed 0-week- mice according to approved Singapore insti al ani hics co ttee (IACUC) protocols. For all animal exp ice ha li access to water. For starvation experim mice v deprived d for 48 hr. In the case of denervation exper s, the ic nerve was incised and mice were maintained for a furthe s. Following the 9 day period, the mice were sacrificed 2 asphyxiation, and various skeletal muscle tissues were collected for t experiments.

### Cell Culture and Treatments

The primary human myoblasts (hMb15) used in this study were kindly gifted by Drs. Vincent Mouly and Gillian Butler-Browne (Institut de Myologie, France). hMb15 cells were cultured and differentiated to myotubes as previously described (Lokireddy et al., 2011b; McFarlane et al., 2011). H9c2 rat cardiomyocytes, gifted by Dr Siu Kwan Sze, Nanyang Technological University, Singapore, and 293T cells (ATCC, USA) were grown in DMEM media containing 10% fetal bovine serum (FBS) and 1% penicillin/streptomycin. Murine C2C12 myoblasts (ATCC, USA) were handled as described previously (Lokireddy et al., 2011a). For treatment experiments, C2C12 myoblasts and myotubes were exposed to either control (dialysis buffer) or 25 μM of Dexamethasone (Dex) (dissolved in DMEM) (Sigma-Aldrich, USA), bacterially or CHO cell expressed Myostatin (CHO-Mstn), or serum-free DMEM (serum starvation) for 1 day. hMstn was expressed and purified from *E. coli* according to a previously published protocol (McFarlane et al., 2011). Myostatin-expressing CHO cells (CHO-Mstn) were kindly gifted by Se-Jin Lee, Johns Hopkins University, USA. CHO-Mstn cells were propagated, and conditioned media was collected as described previously (Zimmers et al., 2002). CHO-Mstn cell conditioned media was used at a dilution of 1:5 in appropriate media. To block proteasome activity, 10 μM of MG132 (Sigma-Aldrich, USA) was added 12 hr prior to harvesting the cells.

### Mitochondrial Membrane Potential Analysi

Mitochondrial membrane potential was sured by rescence microscopy based on the accumulation of tet hylrhodamine thyl ester (TMRM) fluorescence in C2C12 myob ts or bes, as p reviously described protocols (Gomes et al., ; Irwin et a 03; R hello et al., 2010), with slight modifications d bed in he Supp Experimental Procedures.

### Mitochondrial DNA C Numb r Nucle A Ratio Quantification by R

Relative copy n mtDNA per A ratio was measured using a protocol des ed p sly (Chen et a., 2010). See the Supplemental Experimental Procedures f ils of primers and procedure used.

### Qua ication of Mitophagy

Qu fication of mit phagy was performed according to a previously pu ed protocol ayama et al., 2011; Kogure et al., 2006). See the Sup ental Exper ntal Procedures for detailed procedure.

### Statistical ysis

ical analysis was performed using Student's t test, one-way ANOVA, y ANOVA. All values are expressed as means ± SD. The signifi- nce was assessed and represented as *$p < 0.01$.

## SUPPLEMENTAL INFORMATION

Supplemental Information includes six figures, one table, Supplemental Experimental Procedures, and Supplemental References and can be found with this article at http://dx.doi.org/10.1016/j.cmet.2012.10.005.

## ACKNOWLEDGMENTS

We thank Addgene (Cambridge, USA), for providing RFP-LC3 (Dr. Tamotsu Yoshimori, 21075), EGFP-LC3 (Dr. Karla Kirkegaard, 11546), HA-Foxo1 (pCMV5), HA-Foxo1ADA (pCMV5), GFP-FoxO1, (Dr. Domenico Accili, 12142, 12143, 17551), FLAG-FoxO3a WT, HA-FoxO3 TM (Dr. Michael Greenberg, 8360, 1788), and pcDNA GFP FoxO1 AAA (Dr. William Sellers, 9023) constructs. We would like to thank the Ministry of Education, National Research Foundation and the Agency for Science, Technology, and Research (A*STAR) for funding this project.

Received: April 9, 2012
Revised: July 11, 2012
Accepted: October 18, 2012
Published online: November 6, 2012

## REFERENCES

Bach, D., Pich, S., Soriano, F.X., Vega, N., Baumgartner, B., Oriola, J., Daugaard, J.R., Lloberas, J., Camps, M., Zierath, J.R., et al. (2003). Mitofusin-2 determines mitochondrial network architecture and mitochondrial metabolism. A novel regulatory mechanism altered in obesity. J. Biol. Chem. *278*, 17190–17197.

Bechet, D., Tassa, A., Taillandier, D., Combaret, L., and Attaix, D. (2005). Lysosomal proteolysis in skeletal muscle. Int. J. Biochem. Cell Biol. *37*, 2098–2114.

Bodine, S.C., Stitt, T.N., Gonzalez, M., Kline, W.O., Stover, G.L., Bauerlein, R., Zlotchenko, E., Scrimgeour, A., Lawrence, J.C., Glass, D.J., and Yancopoulos,

G.D. (2001). Akt/mTOR pathway is a crucial regulator of skeletal muscle hypertrophy and can prevent muscle atrophy in vivo. Nat. Cell Biol. *3*, 1014–1019.

Braschi, E., Zunino, R., and McBride, H.M. (2009). MAPL is a new mitochondrial SUMO E3 ligase that regulates mitochondrial fission. EMBO Rep. *10*, 748–754.

Chen, H., McCaffery, J.M., and Chan, D.C. (2007). Mitochondrial fusion protects against neurodegeneration in the cerebellum. Cell *130*, 548–562.

Chen, H., Vermulst, M., Wang, Y.E., Chomyn, A., Prolla, T.A., McCaffery, J.M., and Chan, D.C. (2010). Mitochondrial fusion is required for mtDNA stability in skeletal muscle and tolerance of mtDNA mutations. Cell *141*, 280–289.

Clarke, B.A., Drujan, D., Willis, M.S., Murphy, L.O., Corpina, R.A., Burova, E., Rakhilin, S.V., Stitt, T.N., Patterson, C., Latres, E., and Glass, D.J. (2007). The E3 Ligase MuRF1 degrades myosin heavy chain protein in dexamethasone-treated skeletal muscle. Cell Metab. *6*, 376–385.

Cohen, S., Brault, J.J., Gygi, S.P., Glass, D.J., Valenzuela, D.M., Gartner, C., Latres, E., and Goldberg, A.L. (2009). During muscle atrophy, thick, but not thin, filament components are degraded by MuRF1-dependent ubiquitylation. J. Cell Biol. *185*, 1083–1095.

Dodson, S., Baracos, V.E., Jatoi, A., Evans, W.J., Cella, D., Dalton, J.T., and Steiner, M.S. (2011). Muscle wasting in cancer cachexia: clinical implications, diagnosis, and emerging treatment strategies. Annu. Rev. Med. *62*, 265–279.

Emery, A.E. (2002). The muscular dystrophies. Lancet *359*, 687–695.

Evans, W.J. (2010). Skeletal muscle loss: cachexia, sarcopenia, and inactivity. Am. J. Clin. Nutr. *91*, 1123S–1127S.

Gegg, M.E., Cooper, J.M., Chau, K.Y., Rojo, M., Schapira, A.H., and Taanman, J.W. (2010). Mitofusin 1 and mitofusin 2 are ubiquitinated in a PINK1/parkin-dependent manner upon induction of mitophagy. Hum. Mol. G… 4861–4870.

Geisler, S., Holmström, K.M., Skujat, D., Fiesel, F.C., Rothfuss, O.C., …le, P.J., and Springer, W. (2010). PINK1/Parkin-mediated mitophagy is d… dent on VDAC1 and p62/SQSTM1. Nat. Cell Biol. *12*, 1…

Gomes, L.C., Di Benedetto, G., and Scorrano, L… 1). Du… autopha… mitochondria elongate, are spared from degrad… and sus… cell viabilit… Nat. Cell Biol. *13*, 589–598.

Irwin, W.A., Bergamin, N., Sabatelli, P., R…ni, C., I…ian, A., Merlini, L., Braghetta, P., Columbaro, M., Vol…o., Bressan, … et al. (2003). Mitochondrial dysfunction and ap… myopathic mic… collagen VI deficiency. Nat. Genet. *35*, 367–3…

Kambadur, R., Sharma, M…ith, T.P., and … J.J. (1997). Mutations in myostatin (GDF8) in do… muscled Belgian Bl… Piedmontese cattle. Genome Res. *7*, 910–…

Katayama, H., Kog… T., Mi…ima, N., Yoshimori, T., and Miyawaki, A. (2011). A sensitive and … ive techni… for detecting autophagic events based on ly… l deliv… hem. R… *8*, 1042–1052.

Kogure … Kara…a, S., A… aito, K., Kinjo, M., and Miyawaki, A. (2006). …luoresc… variant of a… tein from the stony coral Montipora facilitate… l-colo… fluorescence cross-correlation spectroscopy. Nat. Bi… *24*, 57…

Lecker, S.… 003). Ubiquitin-protein ligases in muscle wasting: multiple parallel pathw… Curr. Opin. Clin. Nutr. Metab. Care *6*, 271–275.

Lee, S.J., and Mc…herron, A.C. (2001). Regulation of myostatin activity and muscle growth. Proc. Natl. Acad. Sci. USA *98*, 9306–9311.

Li, W., Bengtson, M.H., Ulbrich, A., Matsuda, A., Reddy, V.A., Orth, A., Chanda, S.K., Batalov, S., and Joazeiro, C.A. (2008). Genome-wide and functional annotation of human E3 ubiquitin ligases identifies MULAN, a mitochondrial E3 that regulates the organelle's dynamics and signaling. PLoS ONE *3*, e1487. http://dx.doi.org/10.1371/journal.pone.0001487.

Lin, J., Handschin, C., and Spiegelman, B.M. (2005). Metabolic control through the PGC-1 family of transcription coactivators. Cell Metab. *1*, 361–370.

Lokireddy, S., McFarlane, C., Ge, X., Zhang, H., Sze, S.K., Sharma, M., and Kambadur, R. (2011a). Myostatin induces degradation of sarcomeric proteins through a Smad3 signaling mechanism during skeletal muscle wasting. Mol. Endocrinol. *25*, 1936–1949.

Lokireddy, S., Mouly, V., Butler-Browne, G., Gluckman, P.D., Sharma, M., Kambadur, R., and McFarlane, C. (2011b). Myostatin promotes the wasting of human myoblast cultures through promoting ubiquitin-proteasome pathway-mediated loss of sarcomeric proteins. Am. J. Physiol. Cell Physiol. *301*, C1316–C1324.

Mammucari, C., Milan, G., Romanello, V., Masie… f, R., Del Piccolo, P., Burden, S.J., Di Lisi, R., Sandri, C., Zhao… et al. (20… oxO3 controls autophagy in skeletal muscle in vivo. Cell … p. *6*, 458–47…

Masiero, E., Agatea, L., Mammucari, C., Bla… B., Loro, E., …matsu, M., Metzger, D., Reggiani, C., Schiaffi… S., and … M. (2… Autophagy is required to maintain muscle … Cell Metab. *…*

McFarlane, C., Plummer, E., …omas, M…ennebry, A…shby, M., Ling, N., Smith, H., Sharma, M., and K…d… (2006). M…yostatin induces cachexia by activating the u…in p…ic syste… through an NF-kappaB-independent, FoxO… pendent m…ism… ell. Physiol. *209*, 501–514.

McFarlane, C., …Amanda, W.Z…, H.Y., Lokireddy, S., Xiaojia, G., Mouly, V., Bu…-Brow…, Gluckman, P.D., Sharma, M., and Kambadur, R. (2011). Human myostatin … tively regulates human myoblast growth and differ… Am. J. Physi… Physiol. *301*, C195–C203.

N…mura, N., Kimura, Y., Tokuda, M., Honda, S., and Hirose, S. (2006). M…CH-V is a no… mitofusin 2- and Drp1-binding protein able to change m…chondrial mor…ogy. EMBO Rep. *7*, 1019–1022.

O'… M.F., an…ood, D.A. (2009). Denervation-induced oxidative stress and a…naling in muscle. Autophagy *5*, 230–231.

Park, Y.E., Hayashi, Y.K., Bonne, G., Arimura, T., Noguchi, S., Nonaka, I., and … L. (2009). Autophagic degradation of nuclear components in mam…alia…ells. Autophagy *5*, 795–804.

Romanello, V., Guadagnin, E., Gomes, L., Roder, I., Sandri, C., Petersen, Y., Milan, G., Masiero, E., Del Piccolo, P., Foretz, M., et al. (2010). Mitochondrial fission and remodelling contributes to muscle atrophy. EMBO J. *29*, 1774–1785.

Sandri, M., Sandri, C., Gilbert, A., Skurk, C., Calabria, E., Picard, A., Walsh, K., Schiaffino, S., Lecker, S.H., and Goldberg, A.L. (2004). Foxo transcription factors induce the atrophy-related ubiquitin ligase atrogin-1 and cause skeletal muscle atrophy. Cell *117*, 399–412.

Soriano, F.X., Liesa, M., Bach, D., Chan, D.C., Palacín, M., and Zorzano, A. (2006). Evidence for a mitochondrial regulatory pathway defined by peroxisome proliferator-activated receptor-gamma coactivator-1 alpha, estrogen-related receptor-alpha, and mitofusin 2. Diabetes *55*, 1783–1791.

Temiz, P., Weihl, C.C., and Pestronk, A. (2009). Inflammatory myopathies with mitochondrial pathology and protein aggregates. J. Neurol. Sci. *278*, 25–29.

Youle, R.J., and Narendra, D.P. (2011). Mechanisms of mitophagy. Nat. Rev. Mol. Cell Biol. *12*, 9–14.

Zhang, B., Huang, J., Li, H.L., Liu, T., Wang, Y.Y., Waterman, P., Mao, A.P., Xu, L.G., Zhai, Z., Liu, D., et al. (2008). GIDE is a mitochondrial E3 ubiquitin ligase that induces apoptosis and slows growth. Cell Res. *18*, 900–910.

Zhao, J., Brault, J.J., Schild, A., Cao, P., Sandri, M., Schiaffino, S., Lecker, S.H., and Goldberg, A.L. (2007). FoxO3 coordinately activates protein degradation by the autophagic/lysosomal and proteasomal pathways in atrophying muscle cells. Cell Metab. *6*, 472–483.

Zhou, X., Wang, J.L., Lu, J., Song, Y., Kwak, K.S., Jiao, Q., Rosenfeld, R., Chen, Q., Boone, T., Simonet, W.S., et al. (2010). Reversal of cancer cachexia and muscle wasting by ActRIIB antagonism leads to prolonged survival. Cell *142*, 531–543.

Zimmers, T.A., Davies, M.V., Koniaris, L.G., Haynes, P., Esquela, A.F., Tomkinson, K.N., McPherron, A.C., Wolfman, N.M., and Lee, S.J. (2002). Induction of cachexia in mice by systemically administered myostatin. Science *296*, 1486–1488.